npj | Quantum Materials

www.nature.com/npjquantmats

REVIEW ARTICLE OPEN

Check for updates

Materials with strong spin-textured bands

Zhaoliang Liao[1], Peiheng Jiang[2,3], Zhicheng Zhong[2,3,4]✉ and Run-Wei Li[2,3,4]

The materials that exhibit strong spin-textured bands are rapidly attracting more and more attention in past few years. In this new class of quantum materials, the band structures are strongly influenced by spin/magnetization direction, affording new twist to control topological behaviors, quantum anomalous Hall effect, transport, and optical properties by rotating the spin/magnetization. The control of spin direction in spin-textured band materials can be considered as a fundamentally new route toward desired properties compared with conventional spin ordering control. In this article, we will review the research progress on spin-textured band materials from both theoretical and experimental aspects, providing the critical ingredient of this new type of materials, united theory, challenging, and perspective for future research.

npj Quantum Materials (2020)5:30 ; https://doi.org/10.1038/s41535-020-0233-5

INTRODUCTION

Spin is the cornerstone of condensed matter physics. The arrangement and orientation of the spins in a material not only directly determine the magnetic properties, but also strongly affect other physical properties, such as the transport, optical, and thermal properties[1–7]. The magnet, which has enormous application in modern electronics, arises from long-range ferromagnetic ordering structure in which spins spontaneously align parallel to each other. On the contrary, the spontaneously antiparallel alignment of spin leads to anti-ferromagnetism. In between parallel or antiparallel alignment, there are non-collinear spin structures, such as canted or twisting spin structures. The magnetic skyrmion is one of the typical twisting spin textures[5]. Magnetic ordering can also have profound impact on macroscopic properties. For example, the antiferromagnetic (AFM) ordering that can induce a folding of the Brillouin zone and then open a bandgap triggers a Slater-type metal-to-insulator transition[8]. In correlated manganites, the metallic phase is coupled to long-range ferromagnetic ordering and magnetic phase transition from ferromagnetism to para/antiferro-magnetism will trigger a metal-to-insulator transition[2].

The spin orientation, which is another important nature of spin and is usually emphasized by anisotropic response of a material to external magnetic field, is also vital for many physical phenomena. The orientation of the spin in a magnet can be stabilized to a specific direction owing to magnetic anisotropy[9]. Rotating the magnetization direction leads to many novel magneto-phenomena (Fig. 1), such as spin-orbit interaction driven anisotropic magnetoresistance (AMR)[10], giant magnetoresistance in ferromagnet/nonmagnet/ferromagnet sandwiched structure[6], anomalous Hall effect[11], magneto-optic Kerr effect[12,13], and magnetostriction[14,15], etc. The functionality of compass roots in magnetic anisotropy energy which stabilizes spin along a specific crystal axis, and thus this axis, which is defined as magnetic easy axis, mechanically aligns along the magnetic field of the earth. Either AMR in a material or giant magnetoresistance in a sandwiched device, the spin-dependent scattering rules the underlying physics[6,10]. However, no matter the magnetic anisotropy energy[9], spin-dependent scattering[6,10], or spin-dependent light matter interaction[12,13], a change of the spin direction does not fundamentally alters a material's electronic phase, in strong contrast to spin ordering driven electronic phase transition in many correlated materials. The proposed quantum compass material, in which exchange coupling between spins is spatially dependent on the spin direction, though can generate many spin-orientation-dependent novel electronic phase, is still a matter of theory[16].

The giant spin-textured band materials, which have been predicted by theory and experimentally demonstrated in past several years[17–20], make the spin orientation in the spotlight of condensed matter physics. In this new class of quantum materials, rotating the spin direction significantly varies the band structure by an energy scale of one order of magnitude larger than traditional Zeeman splitting, and consequently induces a large variation of physical properties and gives rise to many unprecedented phenomena (Fig. 1, left). Typical examples include the theoretically predicted spin orientation controlled direct-to-indirect bandgap transition in CrI_3[17], quantum anomalous Hall with in-plane magnetization in LaCl[21], topological phase transitions in AFM van der Waals material $MnBi_2Te_4$[22], and switchable Weyl nodes in Kagome ferromagnetic Fe_3Sn_2[23]. More excitingly, several experiments already demonstrated the effect of strong dependence of band structures on the magnetization directions in a couple of materials, e.g., magnetization vector governed symmetry of Fermi surface in Fe_3Sn_2 probed by scanning tunneling microscopy (STM) and spectroscopy (STS)[18]. This new type of quantum materials affords many advantages for application in electronic devices and can be a realistic system in parallel to quantum compass materials[17]. Compared with the control of spin ordering, the direction of the spin can be readily manipulated by external magnetic field, rendering the spin-textured band materials applicable for spintronics[17,20]. The giant response of physical properties to magnetic field further makes it a promising sensor to map magnetic field vector.

Many novel physical phenomena together with promising applications in next-generation electronics are bringing more and more intense focus on spin-textured band materials. Theoretically, spin-vector-dependent spin-orbit coupling (SOC), which changes

[1]National Synchrotron Radiation Laboratory, University of Science and Technology of China, Hefei 230026, China. [2]CAS Key Laboratory of Magnetic Materials and Devices, Ningbo Institute of Materials Technology and Engineering, Chinese Academy of Sciences, Ningbo 315201, China. [3]Zhejiang Province Key Laboratory of Magnetic Materials and Application Technology, Ningbo Institute of Materials Technology and Engineering, Chinese Academy of Sciences, Ningbo 315201, China. [4]China Center of Materials Science and Optoelectronics Engineering, University of Chinese Academy of Sciences, Beijing 100049, China. ✉email: zhong@nimte.ac.cn

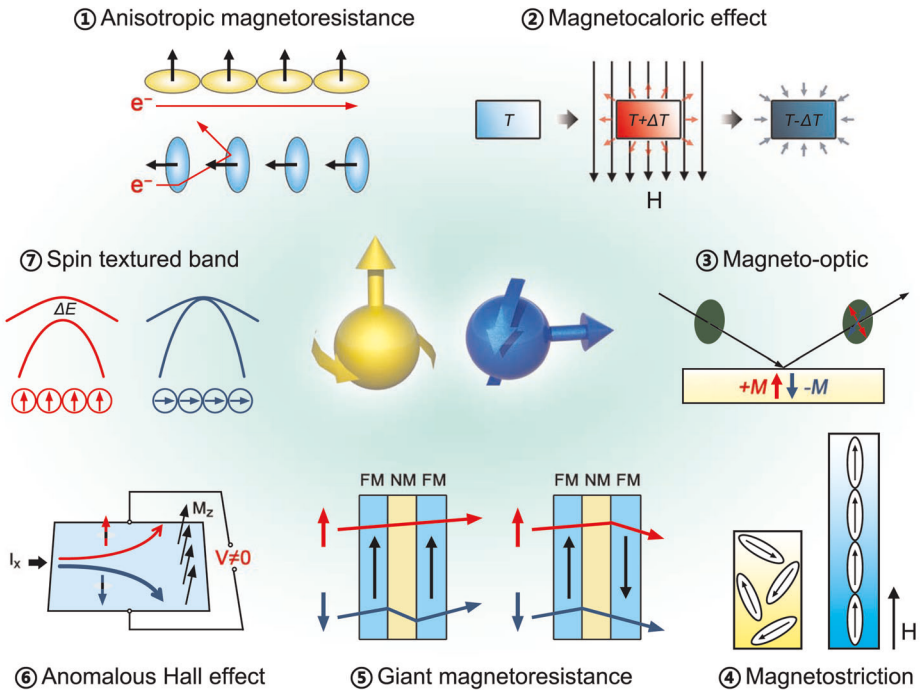

Fig. 1 Magnetization direction controlled physical properties.

the electron Bloch wave is one central ingredient to induce spin-textured band[17,23–26]. In this review, we summarize recent progress in this rapid developing new field in order to provide the critical ingredients of this new type of materials, united theory, challenging and perspective for future research. We will start in Sec II by introducing the theory on spin-textured band materials where the central role of SOC and symmetry breaking is addressed. Next in Sec III, we discuss the experimental reports on spin-textured materials and their connection to theory prediction. Finally in Sec IV, a summary and perspective are given.

THEORY OF SPIN-TEXTURED BAND MATERIALS

Toy models

In correlated materials, spin, charge, and orbital are all active degrees of freedom and their delicate coupling is essential for the diverse electronic phases. Among these internal degrees of freedoms, spin ($\vec{S}$) and orbital ($\vec{L}$) are vector components, thereby serving as indispensable components for developing compass materials where the vector of a component can significantly influence the band structures and properties. The orbital that can be controlled through lattice distortion has been demonstrated in the past in many correlated materials to effectively change the electronic properties[27]. Unfortunately, dynamic lattice control is hardly accessible, hindering practical device application. The spin, which though is easily manipulated by either magnetic field through Zeeman effect or electric field through magnetoelectric coupling[28,29], has global SU(2) symmetry and in many circumstance has isotropic coupling. This peculiarity stands in the way of developing spin vector governed electronic phases.

In a situation where SOC is very strong, however, the spin is intensely entangled with orbital degree of freedom. As a result, the spin is no longer a good quantum number and is not dictated by SU(2) symmetry, making a material with strong SOC drastically differs from other systems with negligible SOC and exhibit many novel phenomena[30], such as topological surface states, photogalvanic effect, chiral domain wall, and spin-charge conversion. Another important ingredient to strength the role of spin direction is to reduce the lattice symmetry, which can maximize the SOC anisotropy. Last but not least, magnetically coupled spins are essential to provide collective behavior from spin degree of freedom and to produce distinct effect on band structures. With these three ingredients, a toy model based on a two-dimensional ferromagnetic material is introduced to illustrate the influence of spin orientation on band structure. The Hamiltonian is described by $H = H_0(k) + \left(\frac{\lambda}{2}\right)\sigma(\theta,\varphi) + \xi \boldsymbol{L}\cdot\boldsymbol{S}$[31]. Here, $H_0(k)$ is the paramagnetic tight-binding Hamiltonian with matrix elements $H_{\alpha\beta} = \sum_{\boldsymbol{R}} t_{\alpha\beta}(\boldsymbol{R}) e^{i\boldsymbol{K}\cdot\boldsymbol{R}}$. The term $t_{\alpha\beta}(\boldsymbol{R})$ represents a hopping integral from orbital α to orbital β with lattice spacing $\boldsymbol{R}$, and $\boldsymbol{K}$ is the wave vector. The second term $\left(\frac{\lambda}{2}\right)\sigma(\theta,\varphi)$ describes an exchange splitting λ with magnetization oriented along a specific direction (θ,φ), and $\sigma(\theta,\varphi)$ is the vector of Pauli matrices. The last term is the SOC and the coefficient ξ is the coupling strength. For simplicity, only p orbitals (p_x, p_y, and p_z) are considered here, but it is worth to note that this toy model can be also used for more complex orbital configuration.

For a 2D ferromagnetic material, it is natural to define the out-of-plane direction as the z direction and in-plane as (x, y). The ferromagnetic exchange interaction shifts the spin down channel to higher energy, unoccupied states. Meanwhile, the $|p_{z\uparrow}\rangle$ orbital (where $\uparrow$ indicates spin up) is split off by 2D confinement effect. Therefore, we mainly focus on $|p_{x\uparrow}\rangle$ and $|p_{y\uparrow}\rangle$ orbitals, which form bands near the Fermi energy. We first consider a situation where the spin is oriented along the out-of-plane direction (M//c). In this case, one has $\langle p_{x\uparrow}|\boldsymbol{L}\cdot\boldsymbol{S}|p_{y\uparrow}\rangle = -i$. As a result, the Hamiltonian has some non-zero off-diagonal mixing terms and the bands at Γ become non-degenerate. A splitting energy ΔE of ~200 meV is found at the Γ point when $\xi = 100$ meV is used for calculation (see Fig. 2a). This energy splitting is indeed induced by SOC, as the splitting disappears if the SOC is not included (e.g., $\xi = 0$). In contrast to the situation of M//c, the off-diagonal term $\langle p_{x\rightarrow}|\boldsymbol{L}\cdot\boldsymbol{S}|p_{y\rightarrow}\rangle$ becomes zero ($\rightarrow$ denotes spin up channel along in-plane direction) for M//a. Accordingly, the former splitting is removed and bands at Γ are degenerate as shown in Fig. 2b. As the SOC term $\boldsymbol{L}\cdot\boldsymbol{S}$ continuously changes with rotating the spin from out-of-plane toward in-plane, the SOC-induced gap ΔE gradually decreases with increasing angle of the spin relative to out-of-plane

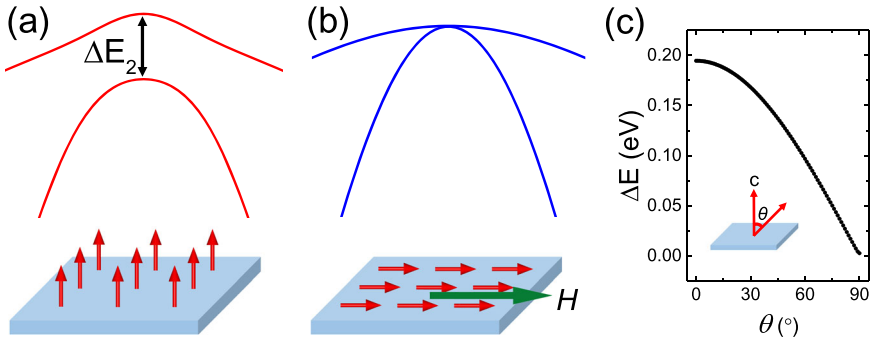

Fig. 2 Schematic view of giant spin-textured band structure effect. Calculated band splitting using toy model for a two-dimensional ferromagnet with **a** magnetization along out-of-plane *c* axis (M//*c*), and **b** rearranged magnetization along in-plane *a* axis (M//*a*) by applying a magnetic field *H*. The energy splitting Δ*E* is on an order of 10^{-1} eV, which is ~10^3 times larger than Zeeman splitting at 1 T. **c** The energy splitting Δ*E* as a function of the angle of spin relative to out-of-plane direction. (**a**, **b**, adapted from ref. [17] with permission, copyright American Chemical Society 2018).

direction, as shown in Fig. 2c. This fact further validates the strong dependence of band structure on spin orientation.

The toy model suggests three criteria for discovering spin-textured band materials: (i) strong SOC to induce non-equivalent electronic behavior for different spin orientations; (ii) a low crystal symmetry that has large crystalline anisotropy to maximize SOC anisotropy; (iii) magnetically coupled electrons to obtain the collective behavior. To illustrate the role of symmetry, the model is extended to a non-layered 3D cubic system where the structure is isotropic. It is found that the change of the band structure at Γ in the 3D case is not observed because of equivalent spin orientations resulting from the high symmetry. These criteria suggest that the most promising candidates are ferromagnetic materials with strong SOC and high crystalline anisotropy. In light of these criteria, a series of promising spin-textured band materials have been predicted in recent 2 years, such as CrI_3[17], Fe_3Sn_2[18,23], Fe_3GeTe_2[19], LaCl[21], $CoGa_2X_4$ (X = S, Se, or Te)[26], Sr_2IrO_4[32], $Co_3Sn_2S_2$[25], $MnBi_2Te_4$[22], $NiTl_2S_4$[33], C_4CrX_3 (X = Ge and Si)[34], and $(Bi, Sb)_2Te_3/Cr_x(Bi,Sb)_{2-x}Te_3$ heterostructure[35].

Spin direction controlled spin-orbit gap

As indicated in the toy model, the spin direction controlled energy splitting in spin-textured band materials should be intimately correlated to SOC. Such an energy splitting could lead to the opening or tuning of the bandgap, i.e., spin-orbit gap. A large spin-orbit gap likely occurs in a material with strong SOC. Several materials with large spin-orbit gap have been predicted previously, and one paradigm is the 2D ferromagnetic CrI_3[17], in which the heavy I element hosts strong SOC and Cr hosts the magnetic coupling. Theoretical calculation suggests that rotating the spin direction of CrI_3 can significantly modify electronic band structures as shown in Fig. 3. In the case of M//*c*, the splitting energies between the two highest valence bands and the two lowest conduction bands at Γ are 174.50 and 64.42 meV, respectively. When the spin lies in-plane, i.e., M//*a*, however, such energy splitting vanishes. As a consequence, the bandgap is tuned from 0.91 eV to 0.96 eV. More importantly, the magnetic moment switching causes a direct-to-indirect bandgap transition.

Another example of spin-orbit gap is found in the 2D ternary chalcogenides, i.e., the $CoGa_2X_4$ (*X* = S, Se, or Te) family[26]. Density functional theory calculations demonstrate that easy plane magnetization is favored in $CoGa_2X_4$. However, the magnetic anisotropic energy between in-plane (easy axis) and out-of-plane (hard axis) magnetization is much smaller than 1 meV, e.g., 0.047 meV for $CoGa_2S_4$. Therefore, magnetization or spin direction can be easily tuned by an external magnetic field. When tuning the magnetization from in-plane to out-of-plane direction, an energy splitting of 32 meV at K point occurs and thus opens a bandgap. As the magnetization direction can be also tuned by applying a tensile strain, the strain is found to affect the spin-orbit gap as well in these ternary chalcogenides.

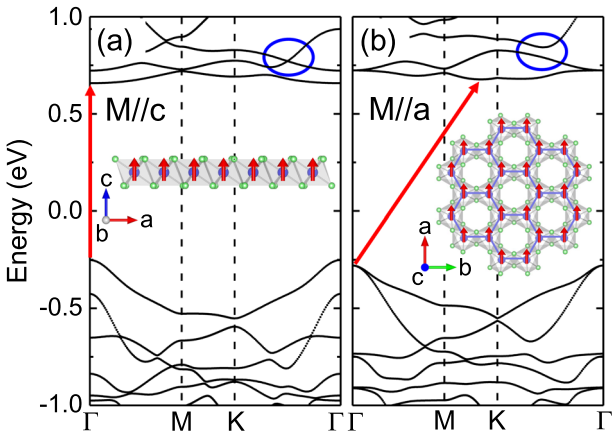

Fig. 3 Spin-orbit gap in monolayer CrI_3. a–b Calculated electronic band structure of ferromagnetic CrI_3 monolayer with **a** spin direction along out-of-plane *c* axis (M//*c*), and **b** in-plane *a* axis (M//*a*). The tuning of spin direction causes three significant changes in electronic band structures, including a direct-to-indirect bandgap transition, change of Fermi surface, and modification of the topological states. (adapted from ref. [17] with permission, copyright American Chemical Society 2018).

Topological phase transition

In magnetic materials, the spin direction has a significant influence on the symmetry of a crystal, and the magnetic symmetry or group is quite complex to address. Here we introduce a simple example in 2D magnetic crystals. In these crystals, the plane symmetry is conserved under out-of-plane spin direction, but is broken for the cases of in-plane spin directions. The change of symmetry can cause large change of electronic band structure at specific k point, e.g., the opening of bandgap at band crossings, and then might result in topological phase transition.

Topological phase transition triggered by change of spin direction has been predicted in 2D ferromagnetic CrI_3[17]. As indicated by blue circles in Fig. 3, the second and third conduction bands of CrI_3 monolayer cross each other without opening a gap along the K-Γ direction for M//*c*. Whereas, the bands cross is broken and a gap is opened when rotating the spin direction to in-plane (M//*a*). Consequently, the topological character of CrI_3 monolayer transforms from Dirac semimetal to Chern topological insulator. Similar behavior was also predicted in 2D LaCl[21]. The 2D

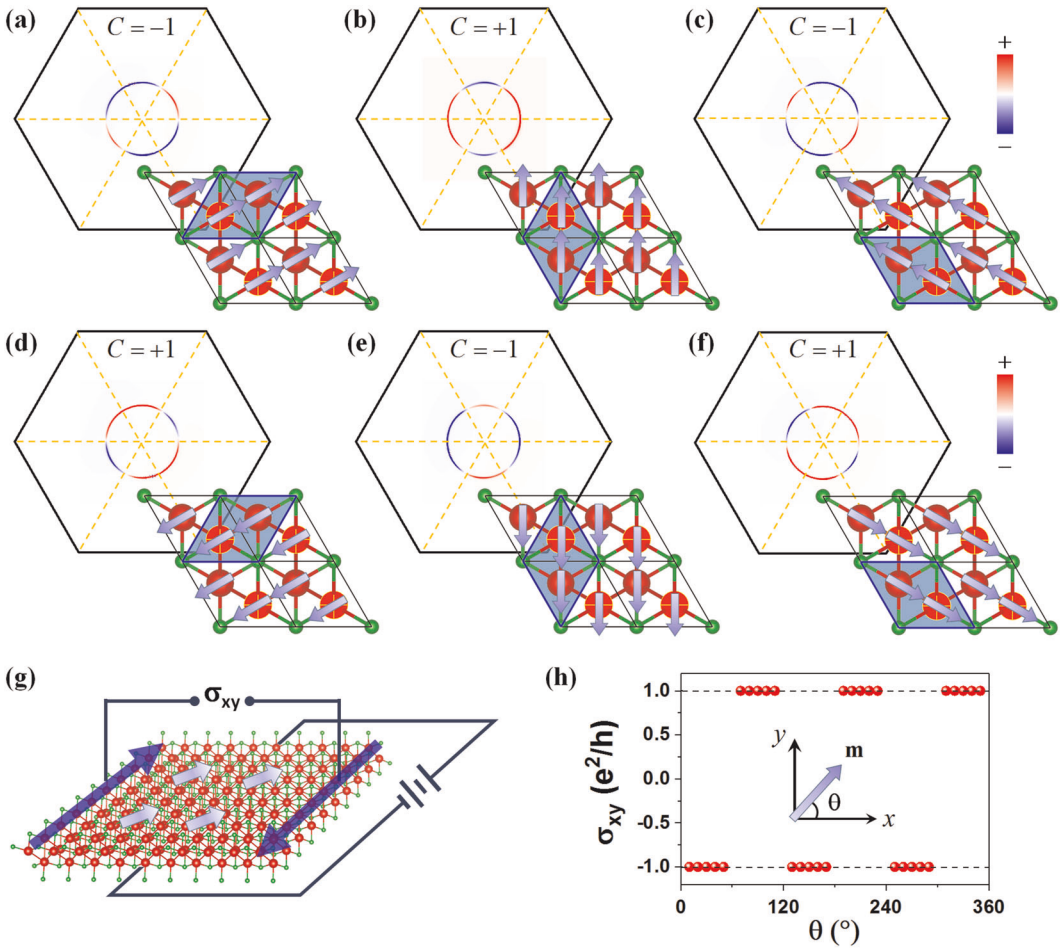

Fig. 4 Quantum anomalous Hall effect in LaCl monolayer. a–f Magnetization direction-dependent Berry curvature and Chern number in LaCl monolayer. **g** Schematic setup of the measurement of quantum anomalous Hall effect and **h** calculated quantized Hall conductivity by varying in-plane magnetization directions. (adapted from ref. [21] with permission, copyright American Physical Society 2018).

LaCl has hexagonal lattice which has three mirror planes. As the magnetization is tuned to different in-plane directions, the mirror symmetry is preserved if the magnetization direction is perpendicular to the mirror plane. Otherwise, the mirror symmetry will be broken. The variation of mirror symmetry under different magnetization directions leads to periodical change of the Chern number in LaCl as shown in Fig. 4a–f. Angle-dependent quantized Hall conductivity with 120° symmetry was also theoretically calculated as shown in Fig. 4h, which could be experimentally confirmed by measuring the Hall at different in-plane magnetization angles as shown in Fig. 4g.

For a newly discovered AFM topological insulator $MnBi_2Te_4$[22,36–41], its van der Waals nature and interlayer AFM coupling suggest that the magnetic order and orientation can be variously changed, e.g., ferromagnetic or AFM order with different spin orientations, by applying magnetic field. Under such a change, the symmetry, orbital hybridization, and band structures can be highly controlled, which leading to various topological phase transitions, such as AFM mirror topological crystalline insulators and type-I topological Weyl semimetals[22].

Furthermore, rotating the magnetization direction has been found to be able to create and control Weyl nodes in several materials, such as Fe_3Sn_2[23], $Co_3Sn_2S_2$[25], and C_4CrX_3 (X = Ge and Si)[34]. Taking the Kagome ferromagnet Fe_3Sn_2 as an example, as its symmetry can be controlled by magnetization direction, the Fe_3Sn_2 exhibits different symmetry operation under different magnetization directions[23]. In detail, the system is protected by space inversion symmetry P, C_{2y}, and the mirror operation M_y for M//y, by space inversion symmetry P for M//x, and by P-symmetry, $C_{3\bar{z}}$, and C_{3z} for M//z. As shown in Fig. 5, the resulted difference in symmetry gives rise to eight pairs, ten pairs, and six pairs Weyl nodes at different points for M//y, M//x, M//z, respectively.

EXPERIMENTS ON SPIN-TEXTURED BAND MATERIALS

As many physical properties are strongly determined by the band structures, manipulation of the band structures by spin rotation is expected to significantly change the physical properties, leading to many novel magneto-phenomena. Taking the CrI_3 as an example, the direct-to-indirect bandgap transition triggered by spin rotated from out-of-plane to in-plane will lead to markedly suppressed photoluminescence[17]. AMR is another important effect in spin-textured band materials, because of that transport property highly depends on the band structure. In the situation that spin-orbit gap is opened at Fermi level, a remarkable spin-direction-driven metal-to-insulator transition can occur, which is worth to be revealed and investigated further in future. The spin reorientation induced topological phase transition and quantum anomalous Hall are another tantalizing phenomena to be revealed experimentally. As these phenomena are sensitive to local band change and do not require large change of the whole band, local modification of the band topologies then can cause huge effect on properties.

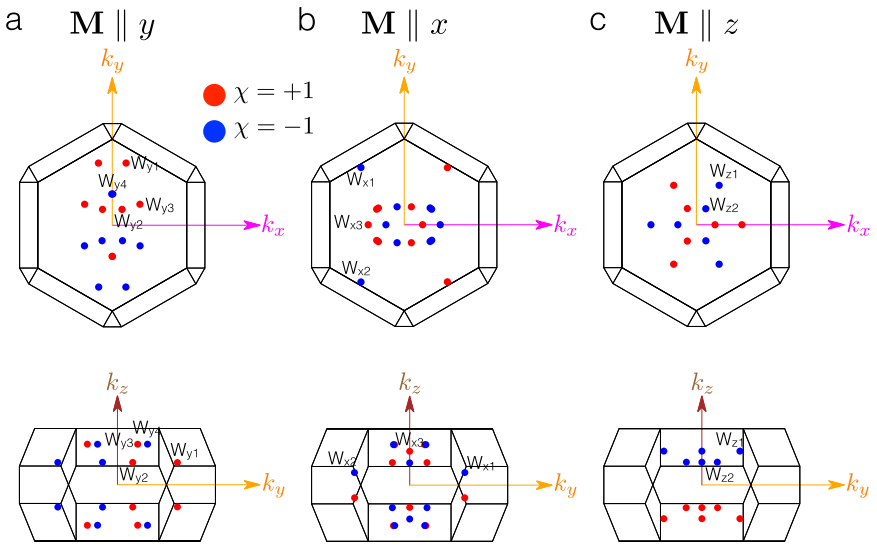

Fig. 5 Creation and control of Weyl nodes via rotating magnetization direction in Fe_3Sn_2. a–c Distribution of Weyl points for magnetization along **a** *y* (M//*y*), **b** *x* (M//*x*), and **c** *z* (M//*z*) directions. Figure is adapted from ref. [23].

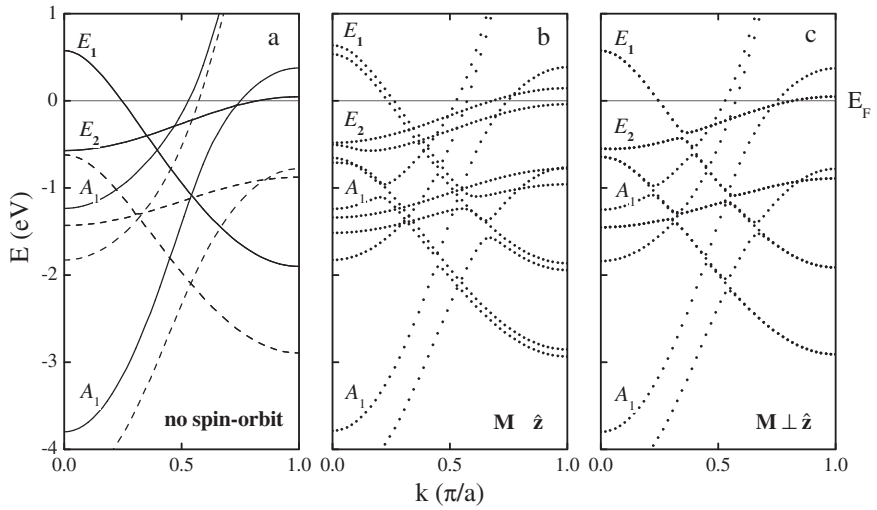

Fig. 6 Calculated band structure of monoatomic Ni wire. a Without SOC and **b** with SOC for magnetization parallel to *z* axis (M//*z*) and **c** with SOC for M⊥*z*. The solid/dashed lines in **a** indicate the minority/majority-spin bands. The irreducible representation (labels in Figure) of the group $C_{\infty v}$ are displayed for minority-spin bands only. (adapted from ref. [45] with permission, copyright American Physical Society 2005).

Ballistic AMR

The first and intuitive glance of incarnation of spin-textured band effect is the AMR. As the magnetic field will induce a Zeeman energy and thus force the spin to align along field direction, a vector field therefore can rotate the spin and change the band structure. Accordingly, the conductivity varies with field direction, leading to AMR. This novel AMR that is owing to the change of Fermi surface is fundamentally different from conventional ARM owing to spin-direction-dependent scattering[10]. The AMR owing to spin-textured band effect was early reported in ballistic anisotropic magnetoresistance (BAMR). With respect to ballistic transport in a ferromagnetic material, the sample dimension is smaller than the mean free path of electrons and the electron conductivity is quantized to $G = Ne^2/h$[42], where *N* is the number of electron sub-bands that cross the Fermi level and *h* is the Planck constant. Change of *N* owing to band structure reconstruction with different magnetization direction is expected to generate quantized magnetoresistance ($\Delta Ne^2/h$). Early experiment in 2002 on Ni ballistic nanocontacts revealed the change of conductance from magnetization parallel to current (m//I) configuration to m⊥I configuration[43]. Later in 2004, Yang et al.[44] found the conductance change ΔG is of the order of e^2/h. Since spin-direction-dependent scattering is not applicable in the situation of ballistic transport any more, the BAMR was theoretically suggested to arise from effect of spin-orbit interaction on the band structure, which is magnetization dependent[45]. Ab-initio calculation by Velev et al.[45] showed a reduction of bands crossing the Fermi energy when magnetization changes from m⊥*z* to m//*z* as shown in Fig. 6. Here the *z* is long axis of ferromagnetic metal nanowires. For m⊥*z*, the structure is nearly the same with situation without considering SOC. However, the SOC removes the spin degeneracy when m//*z* and more significantly the band splitting removes one band from Fermi surface, reducing the conduction channel.

The predicted quantized magnetoresistance in ballistic transport owing to spin-textured band effect has been ambiguously demonstrated by Sokolov et al.[46] in cobalt nanocontact as shown in Fig. 7. A stepwise variation in the ballistic conduction is

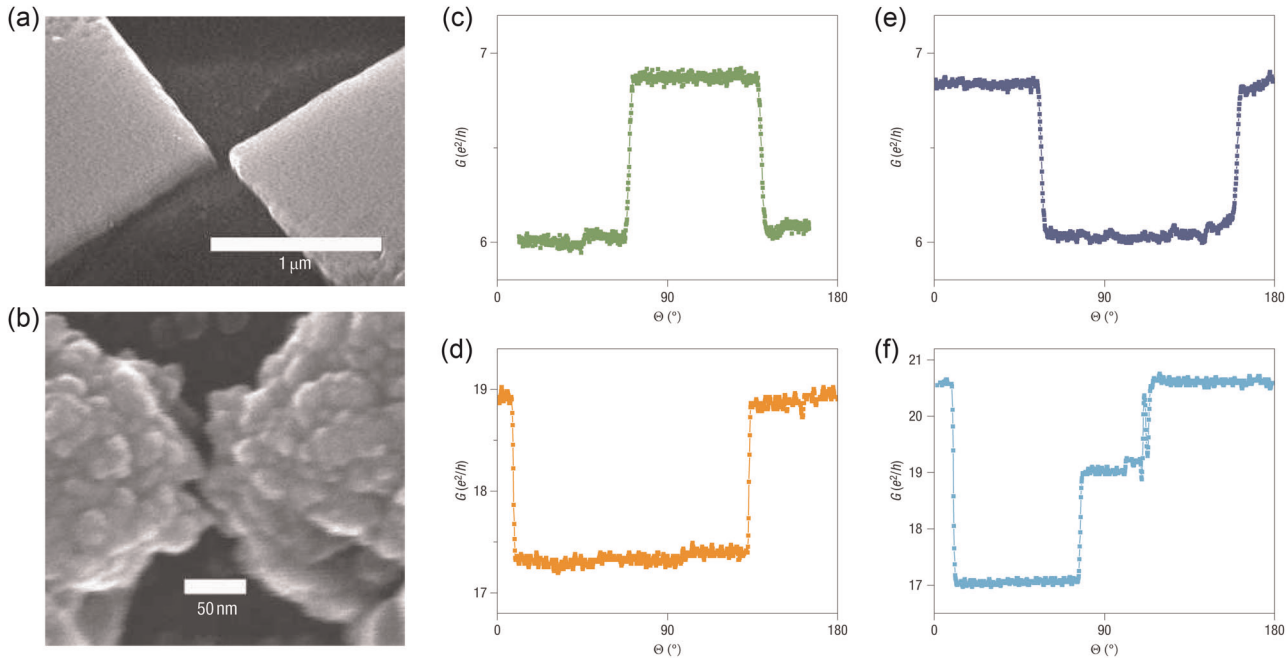

Fig. 7 Ballistic transport in Co nanocontacts. a Images of fabricated arrow-shaped Au electrodes bonded to a Si substrate. **b** High-magnification image of Co contact area between the Au electrodes. **c–f** The ballistic conductance as a function of the angle Θ between the magnetic field and the sample plane for four different samples. (adapted from ref. [46] with permission, copyright Springer Nature 2007).

observed with changing magnetic field angle (Θ) with respect to the plane of the electrode (see Fig. 7). Remarkably, the conduction is quantized into Ne^2/h step, validating not only the feature of ballistic transport, but also corroborating the picture of change of the number of the band crossing Fermi energy owing to magnetization reorientation. The observed stepwise variation with magnetization angle is due to the fact that only the number of the band crossing Fermi energy matters[42].

Strong spin-textured band effect can also occur in AFM ordering materials. This was demonstrated in Ruddlesden-Popper Sr_2IrO_4. The Sr_2IrO_4 contains heavy 5d Ir element, which produces strong SOC and leads to $J_{eff} = 1/2$ Mott state[47,48]. The spin is locked to the tilted IrO_6 octahedra, as a result, each layer has weak net moment and they anti-align to their nearest neighbors[49]. Under external magnetic field, spin-flip transition occurs and Sr_2IrO_4 exhibits weak FM phase. Theory calculation by Lu et al.[32] shows that rotating the axis of the weak FM phase will change bandgap. With magnetic moment m_{Ir}//[100], the band-gap between $J_{1/2}$-LHB and $J_{1/2}$-UHB is 25.9 meV, whereas this bandgap is increased to 35.0 meV when m_{Ir}//[110]. This spin direction-dependent bandgap manifests itself in anomalous anisotropy transport, which shows minima when M//[110] owing to the increased bandgap when the magnetic moment of Ir is forced to align along [110] direction at high field [32].

Anomalous Hall effect

A local non-zero Berry curvature can have profound impact on electronic properties no matter whether the global topological Chern number (the integral of Berry curvature) is non-trivial[50,51]. This fact suggests that local variation of band structure, especially the band crossing and anti-crossing features can have striking physical impact, whereas the global change of band topology is not required. Such characteristics allow us to achieve novel anomalous transport in spin-textured band materials. In a ferromagnetic van der Waals Fe_3GeTe_2, which is suggested to be a nodal-line semimetal, the SOC can lift the degeneracy of the nodal-line and open a spin-orbit gap[19]. In 2D ferromagnetic material, the $H_{SO} = \lambda_{SO}\boldsymbol{L}\cdot\boldsymbol{S}$ can be treated as $\lambda_{SO}L\cdot\langle S\rangle$. As $\langle L_x\rangle = \langle L_y\rangle = 0$ and $\langle L_z\rangle = 3/4\tau_z$, the SOC does not have influence on the band when *S*//*x*(or *y*) and the band remains intact (Fig. 8a). On the contrary, the *S*//*z* will involve the SOC term, which lifts the twofold degeneracy along nodal-line, leading to large Berry curvature (see Fig. 8b). Benefit from the fact that the magnetic easy axis is along *z* axis, the spin moment is aligned parallel to *z* axis, producing large Berry curvature. This effect manifests itself in very large anomalous Hall effect as shown in Fig. 8c. The Fe_3GeTe_2 exhibits extremely large Hall angle $\Theta_{AH}\left(=\frac{\sigma^A_{xy}}{\sigma_{xx}}\right)$ and Hall factor $S_H\left(=\frac{\sigma^A_{xy}}{M}\right)$ simultaneously, which is found to be contributed by Berry curvature rather than skew scattering or side jump.

Direct imaging of spin-textured band

Although BAMR provides substantial evidence of the vector field-controlled band structures, a direct probe of the band structure change is still required to confirm microscopically the effect of spin direction controlled band structures and offer more detail of their underlying physics. Direct probe of band structure changes has been done by STM and angle resolved photoemission spectroscopy (ARPES). This can be traced back to the earlier work done by Bode et al.[52] in 2002 who first revealed a difference of STS of thin Fe film between domain region and domain wall. As STS probes the density of state, the difference indicates band structure change. Given that the spin direction in domain wall rotates gradually from out-of-plane to in-plane and spins within domains lie in-plane, such difference implies a magnetization direction-dependent density of states, which is attributed to magnetization-dependent mixing between minority d_{xy+xz} and minority d_{z^2} orbitals thanks to SOC. This magnetization-direction-dependent tunneling effect, which is termed tunneling anisotropic magnetoresistance (TAMR) is further extended to magnetic tunneling junction, wherein anisotropic magneto-density-of-state causes a spin-valve like tunneling magnetoresistance[53].

Inspired by TAMR effect, direct visualization of the magnetization-dependent band structure is further demonstrated by ARPES[24]. Młyńczak et al. used APRES to probe the surface band

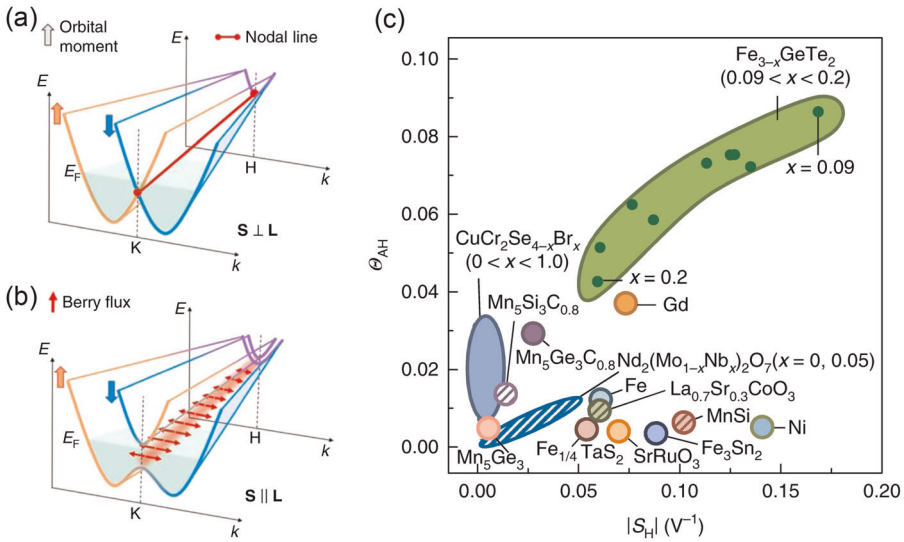

Fig. 8 Schematic illustration of the nodal-line structure along the K-H symmetry line for spin a **perpendicular to orbital *S*⊥*L* and** b **parallel to orbital *S*||*L*.** The thick arrows indicate the opposite orbital momenta *L* along *z*. The opening of spin-orbit gap makes the nodal line behave as 1D vortex line and generates Berry flux in the momentum space as illustrated by the thinner red arrows. **c** Anomalous Hall angle $\Theta_{AH} = \sigma^A_{xy}/\sigma_{xx}$ and anomalous Hall factor $S_H = \sigma^A_{xy}/M$ of $Fe_{3-x}GeTe_2$ and metallic taken at low temperature ($T \ll Tc$) ferromagnets. (adapted from ref. [19] with permission, copyright Springer Nature 2018).

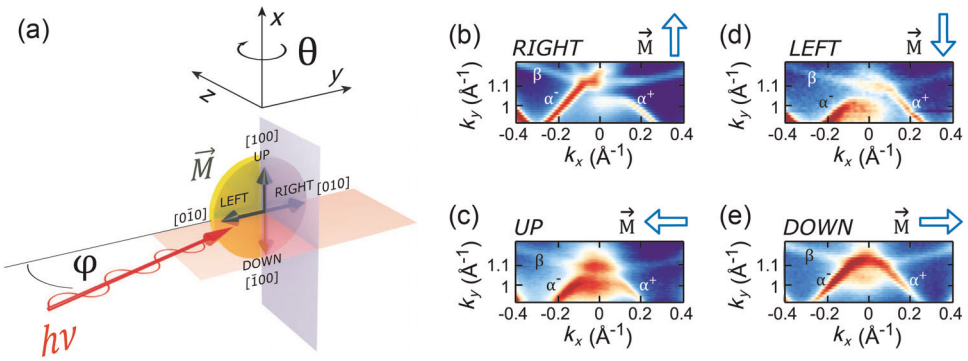

Fig. 9 Probe of magnetization direction dependent band structure by APRES. a Sketch of the experimental ARPES configuration. **b**–**e** Electronic structure of Fe (001) close to the $\bar{X}$ point of the surface Brillouin zone for four different in-plane easy magnetization directions measured at *hv*=16.8eV. Figures are adapted from ref. [24].

structure of a 100 monolayers Fe film on Au (001) single crystal and directly showed the magnetization-dependent spin-orbit gap. As the stray magnetic field from remnant magnetization of this thin Fe film was too weak to distort the photoemission electrons, a true APRES was collected. The ARPES for different magnetization directions are summarized in Fig. 9. A spin-orbit gap is found for magnetization parallel to [010] or [0$\bar{1}$0], whereas this gap closes for magnetization pointing to [100] or [$\bar{1}$00]. The asymmetry between M and −M, e.g., **M**//k_x, **M**//−k_x, is owing to symmetry breaking caused by the presence of magnetization. The field lifts the symmetry and only single mirror plane, which is perpendicular to the magnetization, can be identified and exists. The experimental data can be well fitted into the theory calculation with SOC included[24]. ARPES directly confirms the vector-field-dependent band structure, consistent with aforementioned vector-field-dependent STS and also supported the central role of spin-orbit in spin-textured band materials.

A recent experimental breakthrough on spin-textured band materials comes from the STM study of correlated Kagome magnet Fe_3Sn_2, wherein a spin-driven giant electronic response going beyond Zeeman physics has been confirmed by STM/STS[18]. The conductance spectrum exhibits strong magnetic field direction dependent. Under 1 T field, which is high enough to saturate the magnetization, the side peak (indicated by the blue dots) is found to shift with field angle (see Fig. 10a), following a cosine function $\Delta E = |E - E_{B=0}| = 3.2 - 3.2\cos(2\theta)$. The energy modulation amplitude of 3.2 meV is much larger than Zeeman splitting induced by 1 T magnetic field. The anisotropic vector-field-driven energy shift is mapped into contour surface plot of energy shift ΔE as a function of magnetization vector **M** with a nodal line along *a* axis as shown in Fig. 10b. The *a* axis nodal line arises from the fact that the spontaneous magnetization is along the *a* axis. Owing to strong entanglement between spin space and orbital space, the symmetry of the quasiparticle interference rotates with magnetization direction (see Fig. 10c).

SUMMARY AND FUTURE PERSPECTIVE

Many novel and exciting phenomena have been revealed in spin-textured band materials such as vector-field-controlled Weyl node, semiconductor bandgap, Berry curvature, and Berry phases, opening a new paradigm for discovering new functional materials and novel device applications. A summary of experimentally discovered or theoretically predicted materials with strong

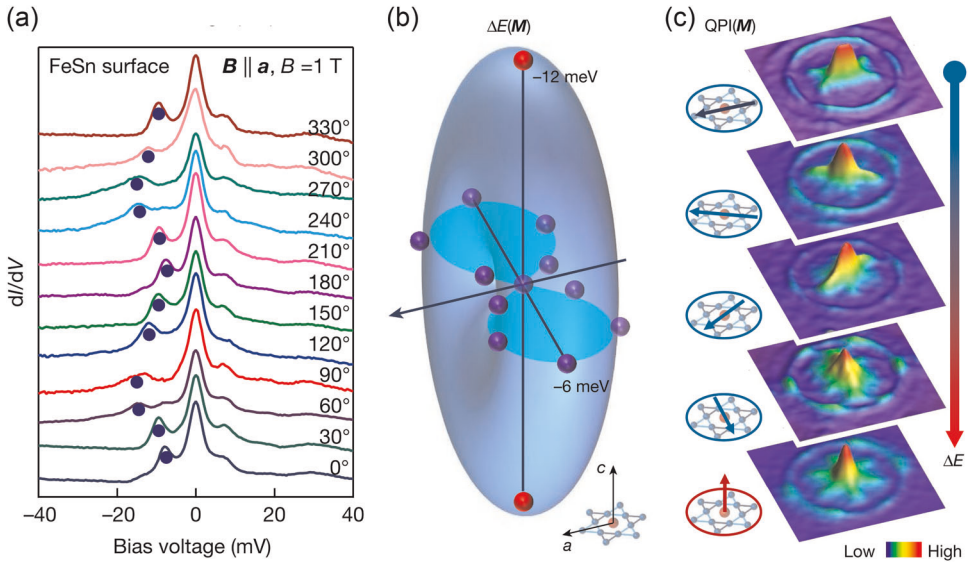

Fig. 10 Vector-magnetization-dependent band structures in Fe_3Sn_2. a The dependence of the scanning tunneling spectra on the angle of in-plane magnetic field relative to *a* axis. **b** 3D mapping of magnetic vector **M** dependent saturated energy shift $\Delta E = E_B - E_{B=0}$. A nodal line exists along the *a* axis. **c** Magnetic field direction dependent pattern of quantum particle interference. The field direction is indicated in the insets with respect to the Kagome lattice. (adapted from ref. [18] with permission, copyright Springer Nature 2018).

Table 1. A summary of spin-textured band materials.

Material	Material type	Tunable property by spin direction
CrI_3	FM	Bandgap
$CoGa_2X_4$		
$MnBi_2Te_4$	AFM TI	Topological phase
$NiTl_2S_4$	AFM	
Fe_3Sn_2	FM metal	Weyl node
$CoSn_2S_2$		
C_4CrX_4	Semimetal	
LaCl	Semimetal	(Anomalous) Hall
Fe_3GeTe_2		
$(Bi,Sb)_2Te_3/Cr_x(Bi,Sb)_{2-x}Te_3$	Magnetic TI	
Sr_2IrO_4	AFM	Anisotropic magnetoresistance

spin-textured bands, spanning many types of functional materials, from semiconductors, ferromagnets, topological insulators, to Weyl metals, are shown in Table 1. The surprisingly wide spectrum of spin-textured bands materials owes to one key feature that spin direction becomes a pivotal knob to tune the band structures. As a result, rotating spin can change the semiconducting bandgap (e.g., CrI_3), Fermi surface topology and symmetry (Fe_3Sn_2), Berry curvature (e.g., Fe_3GeTe_2), and therefore can lead to many emergent spin-direction-triggered electronic phase transition and novel phenomena as summarized in Table 1.

The SOC is one of the well-known spin-direction-dependent interactions that play in the band structure. Besides the tens of materials mentioned in this review, we are expecting to discover more and more spin-textured band materials based on three proposed criteria, including strong SOC, low structural symmetry, and long-range magnetic order, which might be satisfied by many under investigated 2D magnetic materials and other similar materials, as these systems involve heavy elements that hold strong SOC. The large amount of spin-textured band materials and wide spectrum of spin-driven electronic phases strongly suggest the promising application of these materials for diverse applications. It is worth to cultivate the spin-textured band materials to establish new spintronics where spin direction is a key knob.

Regarding that many topological phases and collective competing electronics phases are driven by SOC, many more unprecedented physical properties are yet to be discovered theoretically and experimentally in spin-textured band materials where SOC now can be controlled by spin orientation. Several proposed new phenomena are shown in Fig. 11. In massless Dirac system of graphene, to open the gap is crucial for semiconducting device application. Introducing long-range magnetic ordering and SOC may lead to spin-orbit gap, which can be further controlled by magnetization direction. Such novel phases in graphene can lead to fundamentally new devices combining spintronics and massless Dirac electronics. In addition, if the spin orientation controlled spin-orbit gap is located near Fermi surface, a spin direction controlled metal-to-insulator transition can occur, leading to colossal AMR driven by band structure change. This can be explored in two-dimensional or layer structural ferromagnetic metal. Owing to the coupling of the magnetization to other physical properties, the field-dependent physical properties measurement will not only show the signature of field-magnetization hysteresis loop, such as coercive field and saturation field, but also field orientation dependence, distinguishing the spin-textured band effect from conventional magnetoresistance.

Another exciting system to cultivate the spin-textured band effect is the inversion symmetry breaking where spin up and down lead to two different band structures and hence physical properties. This has big advantage in practical application, as most magnets exhibit spin bistability owing to magnetic anisotropy. The spin is stabilized at direction parallel (S↑) or antiparallel (S↓) to easy axis. If the (S↑) and (S↓) have different band structures and thus different resistances, a non-volatile bi-resistance states then can be realized. We can use this material itself as a non-volatile memory unit. To break the inversion symmetry, we need to explore new types of spin-vector-dependent interaction.

In term of materials candidate for exploring giant spin-textured band effect, oxide heterostructures and van der Waals heterostructures are very promising besides the two-dimensional ferromagnets. Interfacial two-dimensional magnets with strong SOC

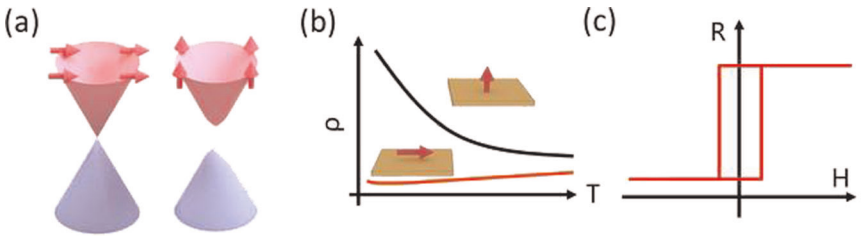

Fig. 11 Examples of expected novel phenomena to be explored in spin-textured band materials. a Gap opening in massless Dirac system. **b** Metal to insulator. **c** Bistable resistance switching.

can be artificially designed and fabricated in heterostructures. In addition, broken inversion symmetry and Rashba SOC can be easily introduced at interface. Therefore, the heterostructures are idea system to explore more exciting phenomena, residing in giant spin-textured band materials.

In summary, intense research has just started and many novel spin-textured band materials have been reported. More exciting phenomena, functionalities, and devices applications need to be cultivated. At the same times, there are still many challenges. The coercive field is very high for many magnets, but the high field is not compatible with ARPES. Therefore, the direct imaging of the band structure change using ARPES is not feasible. The STM faces another technique problem that STM can only probe density of state in conductive samples. New characterization tools and methods, in these regards, are required to be developed to boost the discovery of new spin-textured band materials. Moreover, high throughput theoretical calculation is another promising and efficient route to unearth giant spin-textured band materials.

Received: 16 October 2019; Accepted: 22 April 2020;
Published online: 15 May 2020

REFERENCES

1. Imada, M., Fujimori, A. & Tokura, Y. Metal-insulator transitions. *Rev. Mod. Phys.* **70**, 1039–1263 (1998).
2. Jin, S. et al. Thousandfold change in resistivity in magnetoresistive La-Ca-Mn-O film. *Science* **264**, 413–415 (1994).
3. Hill, N. A. Why are there so few magnetic ferroelectrics? *J. Phys. Chem. B* **104**, 6694–6709 (2000).
4. Eerenstein, W., Mathur, N. D. & Scott, J. F. Multiferroic and magnetoelectric materials. *Nature* **442**, 759–765 (2006).
5. Fert, A., Reyren, N. & Cros, V. Magnetic skyrmions: advances in physics and potential applications. *Nat. Rev. Mater.* **2**, 17031 (2017).
6. Baibich, M. N. et al. Giant magnetoresistance of (001)Fe/(001)Cr magnetic superlattices. *Phys. Rev. Lett.* **61**, 2472–2475 (1988).
7. Wang, Q. et al. Strong interplay between stripe spin fluctuations, nematicity and superconductivity in FeSe. *Nat. Mater.* **15**, 159–163 (2016).
8. Calder, S. et al. Magnetically driven metal-insulator transition in $NaOsO_3$. *Phys. Rev. Lett.* **108**, 257209 (2012).
9. Dieny, B. & Chshiev, M. Perpendicular magnetic anisotropy at transition metal/oxide interfaces and applications. *Rev. Mod. Phys.* **89**, 025008 (2017).
10. Mcguire, T. R. & Potter, R. I. Anisotropic magnetoresistance in Ferromagnetic 3d Alloys. *IEEE Trans. Magn.* **11**, 1018–1038 (1975).
11. Nagaosa, N., Sinova, J., Onoda, S., MacDonald, A. H. & Ong, N. P. Anomalous Hall effect. *Rev. Mod. Phys.* **82**, 1539–1592 (2010).
12. Kerr, J. On rotation of the plane of polarization by reflection from the pole of a magnet. *Philos. Mag.* **3**, 339–343 (1877).
13. Kerr, J. On reflection of polarized light from the equatorial surface of a magnet. *Philos. Mag.* **5**, 161–177 (1878).
14. Joule, J. P. On a new class of magnetic forces. *Ann. Electr. Magn. Chem.* **8**, 219–224 (1842).
15. Lee, E. W. Magnetostriction and magnetomechanical effects. *Rep. Prog. Phys.* **18**, 184–229 (1955).
16. Nussinov, Z. & van den Brink, J. Compass models: theory and physical motivations. *Rev. Mod. Phys.* **87**, 1–59 (2015).
17. Jiang, P., Li, L., Liao, Z., Zhao, Y. X. & Zhong, Z. Spin direction-controlled electronic band structure in two-dimensional ferromagnetic CrI_3. *Nano Lett.* **18**, 3844–3849 (2018).
18. Yin, J. X. et al. Giant and anisotropic many-body spin-orbit tunability in a strongly correlated kagome magnet. *Nature* **562**, 91–95 (2018).
19. Kim, K. et al. Large anomalous Hall current induced by topological nodal lines in a ferromagnetic van der Waals semimetal. *Nat. Mater.* **17**, 794–799 (2018).
20. Tanttu, T. et al. Controlling spin-orbit interactions in silicon quantum dots using magnetic field direction. *Phys. Rev. X* **9**, 021028 (2019).
21. Liu, Z. et al. Intrinsic quantum anomalous Hall effect with in-plane magnetization: searching rule and material prediction. *Phys. Rev. Lett.* **121**, 246401 (2018).
22. Li, J. et al. Magnetically controllable topological quantum phase transitions in the antiferromagnetic topological insulator $MnBi_2Te_4$. *Phys. Rev. B* **100**, 121103 (2019).
23. Yao, M. et al. Switchable Weyl nodes in topological Kagome ferromagnet Fe_3Sn_2. Preprint at https://arxiv.org/abs/1810.01514 (2018).
24. Młyńczak, E. et al. Fermi surface manipulation by external magnetic field demonstrated for a prototypical ferromagnet. *Phys. Rev. X* **6**, 041048 (2016).
25. Ghimire, M. P. et al. Creating Weyl nodes and controlling their energy by magnetization rotation. *Phys. Rev. Res* **1**, 032044 (2019).
26. Zhang, S., Xu, R., Duan, W. & Zou, X. Intrinsic half-metallicity in 2D ternary chalcogenides with high critical temperature and controllable magnetization direction. *Adv. Funct. Mater.* **29**, 1808380 (2019).
27. Tokura, Y. & Nagaosa, N. Orbital physics in transition-metal oxides. *Science* **288**, 462–468 (2000).
28. Yu, G. et al. Switching of perpendicular magnetization by spin-orbit torques in the absence of external magnetic fields. *Nat. Nanotech.* **9**, 548–554 (2014).
29. Matsukura, F., Tokura, Y. & Ohno, H. Control of magnetism by electric fields. *Nat. Nanotech.* **10**, 209–220 (2015).
30. Soumyanarayanan, A., Reyren, N., Fert, A. & Panagopoulos, C. Emergent phenomena induced by spin-orbit coupling at surfaces and interfaces. *Nature* **539**, 509–517 (2016).
31. Liao, Z. et al. Controlled lateral anisotropy in correlated manganite heterostructures by interface-engineered oxygen octahedral coupling. *Nat. Mater.* **15**, 425–431 (2016).
32. Lu, C. et al. Revealing controllable anisotropic magnetoresistance in spin-orbit coupled antiferromagnet Sr_2IrO_4. *Adv. Funct. Mater.* **28**, 1706589 (2018).
33. Liu, J., Meng, S. & Sun, J. T. Spin-orientation-dependent topological states in two-dimensional antiferromagnetic $NiTl_2S_4$ monolayers. *Nano Lett.* **19**, 3321–3326 (2019).
34. Zhang, Z., Gao, Q., Liu, C.-C., Zhang, H. & Yao, Y. Magnetization-direction tunable nodal-line and Weyl phases. *Phys. Rev. B* **98**, 121103 (2018). (R).
35. Kawamura, M. et al. Topological quantum phase transition in magnetic topological insulator upon magnetization rotation. *Phys. Rev. B* **98**, 140404 (2018). (R).
36. Li, J. et al. Intrinsic magnetic topological insulators in van der Waals layered $MnBi_2Te_4$-family materials. *Sci. Adv.* **5**, eaaw5685 (2019).
37. Otrokov, M. M. et al. Unique thickness-dependent properties of the van der Waals interlayer antiferromagnet $MnBi_2Te_4$ films. *Phys. Rev. Lett.* **122**, 107202 (2019).
38. Chen, B. et al. Intrinsic magnetic topological insulator phases in the Sb doped $MnBi_2Te_4$ bulks and thin flakes. *Nat. Commun.* **10**, 4469 (2019).
39. Hao, Y.-J. et al. Gapless surface dirac cone in antiferromagnetic topological insulator $MnBi_2Te_4$. *Phys. Rev. X* **9**, 041038 (2019).
40. Li, H. et al. Dirac surface states in intrinsic magnetic topological insulators $EuSn_2As_2$ and $MnBi_2nTe_{3n+1}$. *Phys. Rev. X* **9**, 041039 (2019).
41. Chen, Y. J. et al. Topological electronic structure and its temperature evolution in antiferromagnetic topological insulator $MnBi_2Te_4$. *Phys. Rev. X* **9**, 041040 (2019).
42. Landauer, R. Spatial variation of currents and fields due to localized scatterers in metallic conduction. *IBM J. Res. Dev.* **1**, 223–231 (1957).
43. Viret, M. et al. Magnetoresistance through a single nickel atom. *Phys. Rev. B* **66**, 220401(R) (2002).

44. Yang, C. S., Zhang, C., Redepenning, J. & Doudin, B. In situ magnetoresistance of Ni nanocontacts. *Appl. Phys. Lett.* **84**, 2865–2867 (2004).
45. Velev, J., Sabirianov, R. F., Jaswal, S. S. & Tsymbal, E. Y. Ballistic anisotropic magnetoresistance. *Phys. Rev. Lett.* **94**, 127203 (2005).
46. Sokolov, A., Zhang, C., Tsymbal, E. Y., Redepenning, J. & Doudin, B. Quantized magnetoresistance in atomic-size contacts. *Nat. Nanotech.* **2**, 171–175 (2007).
47. Cao, G., Bolivar, J., McCall, S. & Crow, J. E. Weak ferromagnetism, metal-to-nonmetal transition, and negative differential resistivity in single-crystal Sr_2IrO_4. *Phys. Rev. B* **57**, 11039–11042 (1998).
48. Kim, B. J. et al. Phase-sensitive observation of a spin-orbital Mott state in Sr_2IrO_4. *Science* **323**, 1329–1332 (2009).
49. Ye, F. et al. Magnetic and crystal structures of Sr_2IrO_4: a neutron diffraction study. *Phys. Rev. B* **87**, 140406 (2013).
50. Xiao, D., Chang, M.-C. & Niu, Q. Berry phase effects on electronic properties. *Rev. Mod. Phys.* **82**, 1959–2007 (2010).
51. Thouless, D. J., Kohmoto, M., Nightingale, M. P. & den Nijs, M. Quantized Hall conductance in a two-dimensional periodic potential. *Phys. Rev. Lett.* **49**, 405–408 (1982).
52. Bode, M. et al. Magnetization-direction-dependent local electronic structure probed by scanning tunneling spectroscopy. *Phys. Rev. Lett.* **89**, 237205 (2002).
53. Gould, C. et al. Tunneling anisotropic magnetoresistance: a spin-valve-like tunnel magnetoresistance using a single magnetic layer. *Phys. Rev. Lett.* **93**, 117203 (2004).

ACKNOWLEDGEMENTS

We gratefully acknowledge financial support from the National Key R&D Program of China (Grants no. 2017YFA0303602) and National Nature Science Foundation of China (Grants no. 11774360, no. 51931011, no. 51525103). Research by Z.L. was financially supported by Hundred Talent Program of the Chinese Academy of Sciences, the Fundamental Research Funds for the Central Universities and National Nature Science Foundation of China (Grants no. 11974325). P.J. was also supported by China Postdoctoral Science Foundation (Grants no. 2018M642497).

AUTHOR CONTRIBUTIONS

The manuscript was written through contributions of all authors.

COMPETING INTERESTS

The authors declare no competing financial or non-financial interests.

ADDITIONAL INFORMATION

Correspondence and requests for materials should be addressed to Z.Z.

Reprints and permission information is available at http://www.nature.com/reprints

Publisher's note Springer Nature remains neutral with regard to jurisdictional claims in published maps and institutional affiliations.